Flavor mixing and time of flight delay of supernova neutrinos

Sandhya Choubey[*] and Kamales Kar[†]
Saha Institute of Nuclear Physics,
1/AF, Bidhannagar, Calcutta 700064, INDIA.

Abstract

The neutrinos from galactic supernovae can be detected by the Sudbury Neutrino Observatory and the Super-Kamiokande. The effect of neutrino mass can show up in the observed neutrino signal by (i) delay in the time of flight and (ii) distortion of the neutrino energy spectrum due to flavor mixing. We discuss a combination of the two effects for both charged and neutral current processes in the detectors for realistic three flavor scenarios and show that neutrino flavor mixing can lead to non-trivial changes in the event rate as a function of time.

[*]e-mail: sandhya@tnp.saha.ernet.in

[†]e-mail: kamales@tnp.saha.ernet.in

I. INTRODUCTION

The subject of neutrino astronomy was firmly established in February 1987 with the detection of neutrinos coming from the explosion of SN1987A in the large magellanic cloud. Ever since there have been lot of activities in this field. Particularly neutrino mass and its implications on supernova neutrino detection have been issues of much discussion. Nonzero neutrino mass was conjectured long ago as a plausible solution to the solar neutrino deficit problem [1] and the atmospheric neutrino anomaly [2,3]. The result from the Super-Kamiokande atmospheric neutrino experiment has finally confirmed that neutrinos are indeed massive [3]. Among the terrestrial accelerator/reactor experiments, only the LSND in Los Alamos has claimed to have seen neutrino mass and mixing [4].

All the three above mentioned evidence for neutrino mass are in a way indirect as they come from neutrino mixing. The direct kinematical measurements of neutrino mass in laboratory experiments at present give extremely poor limits [5,6] which far exceeds the cosmological bound [7]. The other more promising possibility of determining ν_μ/ν_τ masses is through the observation of neutrinos from stellar collapse.

The core of a massive star ($M \geq 8M_\odot$) starts collapsing once it runs out of nuclear fuel. The collapse continues to densities beyond the nuclear matter density after which a bouncing of the infalling matter takes place leading to supernova explosion and the formation of a protoneutron star. Only a small fraction of the huge gravitational energy released in the process goes into the explosion and the rest of the energy is carried away by neutrinos and antineutrinos of all three flavors. These neutrinos for galactic supernova events can be detected by detectors like the Sudbury Neutrino Observatory (SNO) and the Super-Kamiokande (SK). The effect of neutrino mass can show up in the observed neutrino signal in these detectors in two ways,

- by causing delay in the time of flight measurements

- by modifying the neutrino spectra through neutrino flavor mixing

For neutrinos traveling distances ≈ 10 kpc, even a small mass will result in a measurable delay in the arrival time [8–10] resulting in the distortion of the event rate as a function of time. This has been studied extensively before in great detail and the limit that could be put on the ν_τ mass ranged from 10 eV to 200 eV [10].

The postbounce supernova neutrinos are emitted in all the three flavors with ν_μ/ν_τ ($\bar{\nu}_\mu/\bar{\nu}_\tau$) having average energies greater than $\nu_e(\bar{\nu}_e)$. Non-zero neutrino mass and mixing results in more energetic $\nu_\mu/\nu_\tau(\bar{\nu}_\mu/\bar{\nu}_\tau)$ getting converted to $\nu_e(\bar{\nu}_e)$ thereby hardening their resultant energy spectrum and hence enhancing their signal at the detector [11–13]. In a previous work [13] we studied quantitatively the effects of neutrino flavor oscillations on the supernova neutrino spectrum and the number of events at the detector. In this work we make a comparative study of the neutrino signal in the water Cerenkov detectors for a mass range of the neutrinos when both the phenomenon of delay and flavor conversion are operative.

We point out that since the time delay of the massive neutrinos is energy dependent, and since neutrino flavor conversions change the energy spectra of the neutrinos, the time dependence of the event rate at the detector is altered appreciably in presence of mixing. For the mass and mixing parameters we consider two scenarios and substantiate our point

2

by presenting the ratio of the charged to neutral current event rate as a function of time for the different cases. We also study the behavior of the prompt burst neutrinos in presence of delay and mixing. Our study also includes the cases of neutrinos with inverted mass hierarchy and degenerate neutrinos and we comment on the effect on the observed signal for these cases. In section II we briefly describe our model and make predictions for the neutrino signal at the detector for massless neutrinos. In section III we introduce two different mass and mixing scenarios and make a comparative analysis of the cases (a) with delay effects but with zero mixing and (b) with delay along with neutrino flavor conversion. In section IV we consider the effect on the event rate for (a) inverted mass hierarchies and (b) almost degenerate neutrinos. In section V we discuss our results and finally present out conclusions.

II. THE SIGNAL AT THE DETECTOR

The differential number of neutrino events at the detector for a given reaction process is

$$\frac{d^2S}{dEdt} = \sum_i \frac{n}{4\pi D^2} N_{\nu_i}(t)\sigma(E)f_{\nu_i}(E) \tag{1}$$

where i runs over the neutrino species concerned in the given process. One uses for the number of neutrinos produced at the source $N_{\nu_i}(t) = L_{\nu_i}(t)/\langle E_{\nu_i}(t)\rangle$ where $L_{\nu_i}(t)$ is the neutrino luminosity and $\langle E_{\nu_i}(t)\rangle$ is the average energy. In eq.(1) $\sigma(E)$ is the reaction cross-section for the neutrino with the target particle, D is the distance of the neutrino source from the detector (taken as 10kpc), n is the number of detector particles for the reaction considered and $f_{\nu_i}(E)$ is the energy spectrum for the neutrino species involved. By integrating out the energy from eq.(1) we get the time dependence of the various reactions at the detector. To get the total numbers both integrations over energy and time has to be done. We see that the eq.(1) has dependence on two things, the supernova and the detector.

The Supernova:- While for a quantitative analysis people often use numerical supernova model, in this work here we adopt a different point of view. It is seen that among the supernova models there are uncertainties in the inputs and the processes involved and there are differences in the results of the different models as well. We have here considered a profile of the neutrino luminosities and temperatures which have general agreement, though maybe differing in details, with most supernova models. The results that we get are not so sensitive to the details of model predictions and hence are adequate for our purpose.

Most of the numerical supernova models agree that the neutrinos carry away a few times 10^{53} ergs of energy. In this paper we have considered that the total energy radiated by the supernova in neutrinos is 3×10^{53} ergs. This luminosity, which is almost the same for all the neutrino species, has a fast rise over a period of 0.1 sec followed by a slow fall over several seconds. We use a luminosity that has a rise of 0.1 sec using one side of the Gaussian with $\sigma = 0.03$ and then an exponential decay with time constant $\tau = 3$ sec. We have also incorporated the prompt neutrino burst which occurs when the supernova shock crosses the neutrinosphere resulting in the emission of a pure electron neutrino pulse created through electron captures. Again though there are uncertainties in the numerical models regarding the time dependence and the spectrum of this initial ν_e burst, but in general it has a width of $\sim 10^{-2}$ sec, extending between $t \sim 0.04-0.05$ sec postbounce (all times referred to in this

paper are the time after bounce) and a peak height of about 5×10^{53} ergs/sec. The prompt burst neutrinos carry definite energies which reflect the energy spectrum of the captured electrons, which in turn is a Fermi-Dirac with a certain temperature and chemical potential. But to demonstrate the effect, we assume the simple picture, that all the prompt burst neutrinos arrive with a constant energy of 10 MeV.

The average energies associated with the $\nu_e, \bar{\nu}_e$ and ν_μ (the $\nu_\mu, \bar{\nu}_\mu, \nu_\tau$ and $\bar{\nu}_\tau$ have the same energy spectra) are 11 MeV, 16 MeV and 25 MeV respectively in most numerical models. There is again disagreement as to whether the neutrino average energies rise or fall with time. We take them to be constant in time. We have also checked our calculations with linearly time dependent average energies and estimated its effect. The neutrino spectrum is taken to be a pure Fermi-Dirac distribution characterized by the neutrino temperature alone. While most models predict a deviation of the spectrum from a pure black body, the difference is small and does not change our conclusions much.

The Detectors:- We apply our method to two important water Cerenkov detectors, the SK and the SNO. While the former has 50 kton of pure H_2O (fiducial volume is 32 kton), the latter contains 1 kton of pure D_2O surrounded by 8 kton of pure H_2O (fiducial volume of light water is 1.4 kton). For our calculations here we assume that both the detectors have a threshold of 5 MeV above which they detect with 100% efficiency. In Table 1 we give the expected number of events for the various processes involved. All the numbers are for a 1 kton of detector mass and to get the actual numbers one has to multiply them by the fiducial mass [14].

III. THE SIGNAL WITH NON-ZERO MASS

If the neutrinos are massless then the time response at the detector reflect just the time dependence of their luminosity function at the source, which is the same for all flavors and hence the same for the charged current and neutral current reactions. If neutrinos have mass $\sim eV$ then they move at a speed less than the speed of light and hence get perceptibly delayed. For a neutrino of mass m (in eV) and energy E (in MeV), the delay (in sec) in traveling a distance D (in 10 kpc) is

$$\Delta t(E) = 0.515(\frac{m}{E})^2 D \qquad (2)$$

where we have neglected terms second order in (m/E). The time response curve then has contributions from both the luminosity and the mass and hence the shape of the curve changes. If in addition the neutrinos have mixing as well then we have seen [11–13] that the charge current signals go up. This also has an impact on the event rate as a function of time.

The solar neutrino problem, the atmospheric neutrino anomaly and the LSND experiment demand mass and mixing parameters in entirely different ranges. The solar neutrino deficit demands [15] $\Delta m^2 \sim 6.5 \times 10^{-11} eV^2, \sin^2 2\theta \sim 0.75$ (vacuum oscillation solution) or $\Delta m^2 \sim 5 \times 10^{-6} eV^2, \sin^2 2\theta \sim 5.5 \times 10^{-3}$ (non-adiabatic MSW solution), the atmospheric ν_μ depletion is explained by [16,17] $\Delta m^2 \sim 0.005 eV^2, \sin^2 2\theta \sim 1.0$, while LSND gives $\Delta m^2 \sim eV^2, \sin^2 2\theta \sim 10^{-3}$ which is compatible with the mass required for the hot

dark matter in the universe which demands $\sum_i m_{\nu_i}$=few eV [18]. In addition there are constraints coming from r-process nucleosynthesis in the "hot bubble" of the supernova which disfavors the region of the parameter space with $\Delta m^2 > 2eV^2$ and $\sin^2 2\theta > 10^{-5}$ [19]. In order to be able to satisfy all these requirements of the mass and mixing parameters one would need at least 4-generations of neutrinos and perhaps an inverted mass hierarchy as suggested in [20]. We here work with just the three active neutrino flavors with $m_{\nu_e} < m_{\nu_\mu} < m_{\nu_\tau}$ and for the mass and mixing parameters we consider two scenarios.

A. Scenario 1

Here we set $\Delta m_{12}^2 \sim 10^{-6}eV^2$ consistent with the solar neutrino problem and $\Delta m_{13}^2 \approx \Delta m_{23}^2 \sim 1 - 10^4 eV^2$ which is the cosmologically interesting mass range. Here the mixing angle θ_{12} can be constrained from the solar neutrino data and hence we take $\sin^2 2\theta_{12} \sim 10^{-3}$. For θ_{13} there is no experimental data to fall back upon, but from r-process considerations in the "hot bubble" of the supernova we can restrict $\sin^2 2\theta_{13} \sim 10^{-6}$. The atmospheric neutrino anomaly in this case would have to be solved by $\nu_\mu - \nu_s$ oscillations where ν_s is a sterile species and the LSND data would need some explanation other than neutrino oscillations.

In this scenario there will be first a matter enhanced $\nu_e - \nu_\tau$ resonance in the mantle of the supernova followed by a $\nu_e - \nu_\mu$ resonance in the envelope. The two resonances are very well separated and the mixing angle very small, so that the survival probability for an emitted ν_e of energy E in the Landau-Zener approximation is given by [12,21]

$$P_{\nu_e \nu_e} \approx \exp\{-\pi(H_{12}\Delta m_{12}^2 \sin^2 2\theta_{12} + H_{13}\Delta m_{13}^2 \sin^2 2\theta_{13})/4E\} \tag{3}$$

where the H_{12}, H_{13} are the density scale heights at the position of the $\nu_e - \nu_\mu$ and $\nu_e - \nu_\tau$ resonances respectively, given by $H = |\mathrm{d}\ln\rho/\mathrm{d}r|_{\mathrm{res}}^{-1}$. From the density profiles of the mantle and the envelope of a given supernova model, the survival probability for ν_e can be calculated from eq.(3). It has been shown in [22] that for the Δm^2 considered here, both the resonances are completely adiabatic so that there is no level jumping. Even if the jump probability given by eq.(3) is not exactly zero, especially for the $\nu_e - \nu_\mu$ resonance, we expect that the effect will be small and hence for the extremely small mixing angles that we are considering here, we take the survival probability $P_{\nu_e \nu_e} \approx 0$.

As a result of this MSW conversion in the supernova, though the ν_e flux goes down in numbers, it gains in average energy resulting in an enhanced signal at the detector [13]. Of course here since the $\bar{\nu}_e$ do not have any conversion, the $\bar{\nu}_e$ signal remains unaltered. The neutral current events being flavor blind do not show any change either. The shape of the ν_e charged current event rate as a function of time remains the same even though the event rate increases. But the prompt burst neutrinos are absent in the charged current signal if the ν_e get completely converted to ν_μ. The total number of events integrated over time in this scenario with flavor conversion are given in Table 1.

For massive neutrinos with no mixing we will have only delay effects. For the masses assumed here only the ν_τ will be delayed. The expression for the neutral current event rate in the detector is then given by

$$\frac{dS^d_{nc}}{dt} = \frac{n}{4\pi D^2} \int dE\sigma(E)\{N_{\nu_e}(t)f_{\nu_e}(E) + N_{\bar{\nu}_e}(t)f_{\bar{\nu}_e}(E) + 2N_{\nu_\mu}(t)f_{\nu_\mu}(E)$$
$$+ 2N_{\nu_\tau}(t - \Delta t(E))f_{\nu_\tau}(E)\} \tag{4}$$

where dS^d_{nc}/dt denotes the neutral current (nc) event rate with delay (d). Delay therefore distorts the rate vs. time curve. By doing a χ^2 analysis of this shape distortion one can put limits on the mass that can be detected by either of the detectors [10].

If the neutrinos have mass as well as mixing and if we consider complete flavor conversion inside the supernova, then since the ν_μ and the ν_τ spectra are identical, the eq.(4) reduces to,

$$\frac{dS^{do}_{nc}}{dt} = \frac{n}{4\pi D^2} \int dE\sigma(E)\{N_{\nu_e}(t - \Delta t(E))f_{\nu_e}(E) + N_{\bar{\nu}_e}(t)f_{\bar{\nu}_e}(E)$$
$$+ 2N_{\nu_\mu}(t)f_{\nu_\mu}(E) + N_{\nu_\tau}(t)f_{\nu_\tau}(E) + N_{\bar{\nu}_\tau}(t - \Delta t(E))f_{\bar{\nu}_\tau}(E)\} \tag{5}$$

where dS^{do}_{nc}/dt is the reaction rate with delay and flavor conversion.

In fig. 1 we have plotted the neutral current event rate for the reaction ($\nu_x + d \rightarrow n + p + \nu_x$) as a function of time for massless neutrinos along with the cases for mass but no mixing (eq.(4)) and mass along with mixing (eq.(5)). We have used a log scale scale for the time axis to show the prompt burst neutrinos. The figure looks similar for the other neutral current reactions as well, apart from a constant normalization factor depending on the total number of events of the process concerned. The curves corresponding to the massive neutrinos have been given for $m_{\nu_\tau} = 40eV$. As the delay given by eq.(2) depends quadratically on the neutrino mass, the distortion is more for larger masses. From the fig. 1 we see that the prompt neutrino burst shows up at a much later time in presence of delay and complete mixing. For partial conversion ($P_{\nu_e\nu_e} \neq 0$), the prompt burst neutrinos would break up into two, an unconverted ν_e component and a massive component, depending on the value of $P_{\nu_e\nu_e}$ and while the former would arrive undelayed at t$\approx 0.04sec$, the latter component would get delayed by about 8 sec for m_{ν_τ}=40 eV. The comparison of the cases with and without mixing shows that the distortion of the curve due to delay is diluted in the presence of mixing. Although it may seem that the curve with delay and mixing can be simulated by another curve with delay alone but with smaller mass, the actual shape of the two curves would still be different. This difference in shape though may not be statistically significant for the present water Cerenkov detectors.

In fig. 2 we give the ratio R(t) of the total charged current to the neutral current event rate in SNO as a function of time. Plotted are the ratios (i) without mass, (ii) with only mixing, (iii) with delay but zero mixing and (iv) with delay and flavor mixing. The differences in the behavior of R(t) for the four different cases are clearly visible. For no mass R(t)=0.3 and since the time dependence of both the charged current and neutral current reaction rates are the same, their ratio is constant in time. With only mixing the ratio increases appreciably and goes upto R(t)=0.61, remaining constant in time, again due to the same reason. With the introduction of delay the ratio becomes a function of time as the neutral current reaction now has an extra time dependence coming from the mass. At early times as the ν_τ get delayed the neutral current event rate drops increasing R(t). These delayed ν_τs arrive later and hence R(t) falls at large times. This feature can be seen for both the curves with and without mixing. The curve for only delay starts at R(t)=0.52 at t=0sec

and falls to about R(t)=0.26 at t=10sec. For the delay with mixing case the corresponding values of R(t) are 0.83 and 0.51 at t=0 and 10 sec respectively. The noteworthy thing is that the curves with and without mixing are clearly distinguishable and should allow one to differentiate between the two cases of only delay and delay with neutrino flavor conversion.

B. Scenario 2

Here we set $\Delta m_{12}^2 \approx \Delta m_{13}^2 \sim 1 - 10^4 eV^2$ corresponding to the cosmological range and $\Delta m_{23}^2 \sim 10^{-3} eV^2$ which will explain the atmospheric neutrino anomaly. As before we take the mixing angle to be small from r-process considerations. Here we assume that it is the $\nu_e - \nu_s$ mixing which is responsible for the solar neutrino deficit. Though this scheme can accommodate LSND in principle, we will generally consider masses that are higher than the range over which LSND is sensitive.

For a mass spectrum like this, there will be just one matter enhanced resonance in the supernova instead of two as has been numerically shown in [23]. Hence the survival probability for ν_e of energy E in the Landau-Zener approximation is given by

$$P_{\nu_e \nu_e} \approx \exp\{-\pi(H_{13}\Delta m_{13}^2 \sin^2 2\theta_{13})/4E\} \tag{6}$$

and as argued before for adiabatic conversion with small mixing angles we take $P_{\nu_e \nu_e} \approx 0$. The charged current event rate as a function of time and the time integrated number of events in this scenario therefore remains the same as in scenario 1 (see column 3 of Table 1).

For this case both the ν_μ and the ν_τ will be delayed and so the delay effects will be almost twice that we had for the scenario 1. The neutral current time response in the detector for this mass scenario without mixing is given by

$$\frac{dS_{nc}^d}{dt} = \frac{n}{4\pi D^2} \int dE\sigma(E)\{N_{\nu_e}(t)f_{\nu_e}(E) + N_{\bar{\nu}_e}(t)f_{\bar{\nu}_e}(E)$$
$$+ 4N_{\nu_\tau}(t - \Delta t(E))f_{\nu_\tau}(E)\} \tag{7}$$

From the expressions (4) and (7) it is clear that the event rate in scenario 2 with a certain mass m for both ν_μ and ν_τ is not exactly equal to the reaction rate in scenario 1 with a ν_τ mass of $2m$.

If the neutrinos have mass as well as mixing then eq.(7) for complete conversion $P_{\nu_e \nu_e} \approx 0$ becomes

$$\frac{dS_{nc}^{do}}{dt} = \frac{n}{4\pi D^2} \int dE\sigma(E)\{N_{\nu_e}(t - \Delta t(E))f_{\nu_e}(E) + N_{\bar{\nu}_e}(t)f_{\bar{\nu}_e}(E)$$
$$+ 2N_{\nu_\mu}(t - \Delta t(E))f_{\nu_\mu}(E) + N_{\nu_\tau}(t)f_{\nu_\tau}(E) + N_{\bar{\nu}_\tau}(t - \Delta t(E))f_{\bar{\nu}_\tau}(E)\} \tag{8}$$

In fig. 3 we plot as in scenario 1, the $(\nu_x - d)$ event rate as a function of time, for $m_{\nu_\mu} = m_{\nu_\tau} = 40eV$. Clearly the delay effects are more in this case than in scenario 1. The prompt burst neutrinos have a behavior similar to that seen in the scenario 1. In fig. 4 we give the ratio R(t) of the charged current to neutral current reaction rates in SNO as before. All the features that were present earlier are also present here. For no mass R(t)=0.3, which rises to 0.61 on introduction of complete flavor conversion, being constant in time as before.

But here the distortion of the shape of R(t) due to delay is immense. With the introduction of delay the ratio rises to about 1.85 at t=0sec and then falls sharply with time to 0.27 by t=2sec, while for the case of delay with flavor mixing the ratio falls from 1.95 at t=0sec to about 0.57 at t=2sec. Again here the two curves are clearly distinguishable. Also the shape of the R(t) curves in the first 2 seconds are different from the shape of the R(t) curves in the first 2 seconds of scenario 1. This should help us to the distinguish between the two mass patterns considered in scenario 1 and 2.

IV. SIGNAL WITH OTHER MASS PATTERNS

Apart from the ones that we have considered in the previous section, there may be other mass hierarchies for the neutrinos as well. We can have a situation where the neutrino state corresponding to the ν_e is the heaviest mass state [20,24]. Such "inverted" mass hierarchies do not interfere with the r-process in the "hot bubble" [26] though they maybe in conflict with the SN1987A data. The SN1987A analysis of Smirnov, Spergel and Bahcall in [22] constrains $P_{\nu_e \nu_e} \geq 0.65$. But it has been argued by Fuller, Primack and Qian [20] that the constraints from SN1987A are not strong enough and so one may have large resonant antineutrino conversions in the supernova. In Table 1 we report the total signal at the detector for the case $m_{\nu_1} \ll m_{\nu_2} \sim m_{\nu_3}$ with $P_{\nu_e \nu_e} = 0$ in column 4 and with $P_{\nu_e \nu_e} = 0.65$ in column 5.

If ν_es were massive they would get delayed and we would see delay effects in the charged current signal as well. This would create an interesting situation in which the conventional methods suggested in the literature to determine the neutrino mass from the time of flight measurements would fail. But the $^3H\beta$ decay experiments restrict $m_{\nu_e} < 5eV$ [5] (in fact the bound may be even lower [27]). Since the time delay given by eq.(2) depends quadratically on the neutrino mass, the delay effects for such low m_{ν_e} mass is very small. The only signature in this case maybe in the ratio R(t) of the charged current to neutral current event rate in the first 0.2 sec. In the fig. 5 we plot the ratio R(t) in SNO for the various cases as a function of time for $m_{\nu_\mu} \ll m_{\nu_\tau} \sim m_{\nu_e} = 5eV$ and with $P_{\nu_e \nu_e}=0$. For the no mass case R(t)=0.3 which rises to 0.5 when mixing is switched on. For the only delay case the ratio R(t) rises from almost 0.02 initially to about 0.3 at t=0.2sec, the no mass value, beyond which it remains constant. For the case of delay with mixing R(t) rises from 0.25 at t=0.01sec to about 0.5 at t=0.2sec, the only mixing value and remains constant thereafter. The prompt burst neutrinos get delayed in this case even though they do not have flavor conversion here and appear at the same delayed time for charged current and neutral current events.

Instead of hierarchical spectrum, neutrinos may even be almost degenerate with a few eV mass [25]. The small mass splitting between them can account for the solar neutrino problem ($\Delta m^2 \sim 10^{-6}eV^2$) and the atmospheric neutrino anomaly ($\Delta m^2 \sim 10^{-3}eV^2$). This mass pattern does not contradict the r-process as the mass differences here are small and not enough to cause neutrino conversions in the "hot bubble". This scheme of course cannot account for the LSND results. Again here we may have either $m_{\nu_e} < m_{\nu_\mu} < m_{\nu_\tau}$ or $m_{\nu_e} > m_{\nu_\mu} > m_{\nu_\tau}$. While for the former we will have $\nu_e - \nu_\tau$ resonance followed by $\nu_e - \nu_\mu$ resonance, for the latter the antineutrinos will similarly resonate. From the expression (3) one can calculate the relevant probabilities. In this case, for both normal as well as inverted

masses, all the three neutrino species will be delayed. Hence here also we can expect delay effects in both the charged as well as the neutral current events. But here again since m_{ν_e} cannot be larger than 5 eV, the other species will also have a maximum mass of about 5 eV and the delay effects are not large. But again one can expect to see some change in the ratio R(t) of the charged to neutral current event rates as a function of time. In figs. 6 and 7 we plot the ratio R(t) for $m_{\nu_e} < m_{\nu_\mu} < m_{\nu_\tau}$ and $m_{\nu_e} > m_{\nu_\mu} > m_{\nu_\tau}$ respectively with $P_{\nu_e\nu_e} \approx 0$ for the cases with mixing. The prompt neutrino burst appears delayed in both the charged current as well as neutral current signal for the cases where $m_{\nu_e} > m_{\nu_\mu} > m_{\nu_\tau}$. For the $m_{\nu_e} < m_{\nu_\mu} < m_{\nu_\tau}$ the ν_e are transformed to ν_μ and do not appear in the charged current signal, though they do appear at a delayed time in the neutral current events.

V. DISCUSSIONS AND CONCLUSIONS

As the average energies of the $\nu_\mu/\nu_\tau(\bar{\nu}_\mu/\bar{\nu}_\tau)$ are greater than the average energies of the $\nu_e(\bar{\nu}_e)$, neutrino flavor mixing modifies the energy spectrum of the neutrinos. As the detection cross-sections are highly energy dependent this results in the enhancement of the charged current signal, but as the neutral current reactions are flavor blind, the total neutral current signal remains unchanged. However the time delay $\propto 1/E^2$, and as the energy spectrum of the neutrinos change the resultant delay is also modified and this in turn alters the neutral current event rate as a function of time. MSW conversion in the supernova results in de-energising the ν_μ/ν_τ spectra and hence the delay effect should increase. As larger delay caused by larger mass results in further lowering of the neutral current event rate vs. time curve for early times, one would normally expect that the enhanced delay as a result of neutrino flavor conversion would have a similar effect. But the figs. 1 and 3 show that the curves corresponding to delay with mixing are higher than the ones with only time delay. This at first sight seems unexpected. But the point to note is that while the flavor conversion reduces the average energies of the massive ν_x (where x stands for μ/τ) increasing its delay and hence depleting its signal at early times, it energizes the ν_e beam which is detected with full strength. Therefore while for no mixing the ν_x gave the largest signal, for the case with mixing it is the ν_e that assume the more dominant role. If we consider the scenario 1, for the only delay case the delayed ν_τs appear after t$\approx 0.1 sec$, while for delay with flavor conversion the ν_τs appear only after t$\approx 0.5 sec$. So upto t$\approx 0.1 sec$, for only delay we have just the ν_e signal with $\langle E_{\nu_e}\rangle = 11 MeV$ while for delay with mixing we have ν_e signal with $\langle E_{\nu_e}\rangle = 25 MeV$. Hence for t$< 0.1 sec$ the signal for delay with mixing is more as the signal goes up significantly for higher energy neutrinos. Beyond t$\approx 0.1 sec$ the delayed ν_τs start appearing for the only delay case and by t$\approx 0.7 sec$ the signal for only delay becomes equal to the signal for delay with mixing. By this time the delayed ν_τs with $\langle E_{\nu_\tau}\rangle = 11 MeV$ also appear for the delay with mixing case but their contribution is small. By $t \approx 1 sec$ the two curves corresponding to to only delay and delay with mixing approach each other and the difference between them becomes hard to detect.

For scenario 1 and 2 the $\bar{\nu}_e$ spectrum remains unchanged. Hence we can use the large $\bar{\nu}_e$-p signal at SK to fix the supernova model parameters as a function of time. This can then be used to make predictions for the ν_e charged current signal. A comparison of the expected to the actual ν_e signal would give the value of $P_{\nu_e\nu_e}$. This $P_{\nu_e\nu_e}$ can then be incorporated in the analysis and a correct limit for the neutrino mass from the neutral current event rate

9

can be obtained.

On the other hand if the $\bar{\nu}_e$ captures are much larger than most model predictions, then that would indicate a $\bar{\nu}_e$ MSW resonance in the supernova and hence an inverted mass hierarchy. In that case, in principle we would see delay effects in both the neutral as well as the charged current events. But the current laboratory limits on ν_e mass ($m_{\nu_e} \leq 5eV$) ensure that these effects may not be discernible in the present detectors. The neutral current to charged current ratio in the first 0.2 sec could still carry some clue regarding neutrino mass. The other quantity that could in principle be searched for is the prompt neutrino burst. This will appear, if detected, at the same delayed time in the charged and the neutral current signal.

One parameter which carries both the information of the neutrino mass and their mixing is R(t), the ratio of charged to neutral current event rate as a function of time. This ratio as a tool to look for mixing has been suggested before. We have shown here that the shape of R(t) changes in presence of time of flight delay. This shape distortion can be used to put limits on neutrino mass. The ratio is not only sensitive to mass and mixing parameters it is also almost model independent. It is almost independent of the luminosity and depends only on some function of the ratio of neutrino temperatures. We have also repeated our analysis with a linear time dependence for the neutrino temperature and have found that the time dependence of the neutrino temperature does not have much effect on the time dependence of the event rates or the ratio of the charged current to neutral current rates.

We have also studied the prompt neutrino burst under the different possible mass and mixing schemes where one can have perceptible time delay. For normal mass hierarchies with mass and mixing the prompt burst neutrinos are delayed in the neutral current signal and are absent in the ν_e charged current signal. For inverted mass hierarchies the ν_es are delayed but do not undergo flavor conversion and so the prompt burst neutrinos come at the same delayed time for both charged as well as neutral current signal.

In conclusion, we point out that one should consider the delay effects of massive neutrinos with mixing as it has been proved beyond doubt that the neutrinos do mix. We have shown here that neutrino mixing leads to nontrivial changes in the time response of the neutrinos at the detector. The prompt burst neutrinos and the charged current to neutral current ratio are important tools which carry information about the neutrino mass and mixing as demonstrated here and should be studied carefully.

REFERENCES

[1] B.T. Cleveland *et al.*, Astrophys. J. **496**, 505 (1998); Kamiokande Collaboration, K.S. Hirata *et al.*, Phys. Rev. Lett. **77**, 1683 (1996); W. Hampel *et al.*, GALLEX Collaboration, Phys. Lett. **B388**, 384 (1996); D.N. Abdurashitov *et al.*, SAGE Collaboration, Phys. Rev. Lett. **77**, 4708 (1996); Y. Fukuda *et al.*, The Super-Kamiokande Collaboration, Phys. Rev. Lett. **81**, 1158 (1998).

[2] Y. Fukuda *et al.*, The Kamiokande Collaboration, Phys. Lett. **B335**, 237 (1994); R. Becker-Szendy *et al.*, IMB Collaboration, Nucl. Phys. **B38** (Proc. Suppl), 338 (1995); W.W.M. Allison *et al.*, Soudan Collaboration, Phys. Lett. **B391**, 491 (1997); M. Ambrosio *et al.*, MACRO Collaboration, Phys. Lett. **B434**, 451 (1998).

[3] Y. Fukuda *et al.*, The Super-Kamiokande Collaboration, Phys. Lett. **B433**, 9 (1998); Phys. Lett. **B436**, 33 (1998).

[4] C. Athanassopoulos *et al.*, Phys. Rev. Lett. **75**, 2650 (1995); Phys. Rev. Lett. **77**, 3082 (1996); Phys. Rev. Lett. **81**, 1774 (1998).

[5] For ν_e see A.I. Balasev *et al.*, Phys. Lett. **B350**, 263 (1995).

[6] For ν_μ and ν_τ see R.M. Barnett *et al.*, Phys. Rev. **D54**, 1 (1996).

[7] S.S. Gershtein and Y.B. Zeldovich, JETP Lett. **4**, 120 (1966); R. Cowsik and J. Mclelland, Phys. Rev. Lett. **29**, 669 (1972); G.G. Raffelt, *Stars as Laboratories for Fundamental Physics* (University of Chicago Press, 1986), ch 7.

[8] A.S. Burrows, D. Klein, R. Gandhi, Phys. Rev. **D45**, 3361 (1992).

[9] L.M. Krauss *et al.*, Nucl. Phys. **B 380**, 507 (1992).

[10] J.F. Beacom and P. Vogel, Phys. Rev. **D58** , 053010 (1998); Phys. Rev. **D58** , 093012 (1998).

[11] A.S. Burrows, D. Klein, R. Gandhi, Nucl. Phys. **B31** (Proc. Suppl.), 408 (1993).

[12] Y.Z. Qian and G.M. Fuller, Phys. Rev. **D49**, 1762 (1994).

[13] S. Choubey, D. Majumdar, K. Kar, Phys. **G25**, 1001 (1999).

[14] For more details on the detector and the detection processes see [13] and the references therein.

[15] J.N. Bahcall, P.I. Krastev, A. Yu. Smirnov, Phys. Rev. **D58** , 096016 (1998).

[16] Y. Fukuda *et al.*, The Super-Kamiokande Collaboration, Phys. Rev. Lett. **81**, 1562 (1998).

[17] S. Choubey and S. Goswami, preprint hep-ph/9904257.

[18] R.A.C. Croft, W. Hu and R. Dave, preprint astro-ph/9903335.

[19] Y.Z. Qian *et al.*, Phys. Rev. Lett. **71**, 1965 (1993).

[20] G.M. Fuller, J. Primack and Y.Z. Qian, Phys Rev **D52**, 1288 (1995).

[21] T.K. Kuo and J. Panteleone, Phys. Rev. **D 37**, 298 (1988).

[22] A.Yu. Smirnov, D.N. Spergel, J.N. Bahcall, Phys. Rev. **D49**, 1389 (1994).

[23] H.W. Zaglauer and K.H. Schwarzer, Z. Phys. **C40**, 273 (1988).

[24] D.O. Caldwell, R.N. Mohapatra, Phys. Lett. **B354**, 371 (1995); S.M. Bilenky, C. Giunti, C.W. Kim, S.T. Petcov, Phys. Rev. **D54**, 4432 (1996).

[25] J.A. Casas, J.R. Espinosa, A. Ibarra, I. Navarro, preprint hep-ph/9904395.

[26] Y.Z. Qian and G.M. Fuller, Phys. Rev. **D52**, 656 (1995).

[27] V. Lobashev, Pontecorvo Prize lecture at the JINR, Dubna, January 1999.

Table 1 The expected number of neutrino events for a 1 kton water Cerenkov detector. The column A corresponds to massless neutrinos, column B to neutrinos with normal hierarchies ($m_{\nu_e} < m_{\nu_\mu} < m_{\nu_\tau}$) and complete flavor conversion and column C1 and C2 to neutrinos with inverted mass hierarchies ($m_{\nu_e} > m_{\nu_\mu} > m_{\nu_\tau}$). C1 is for $P_{\nu_e\nu_e} = 0$ while C2 is for $P_{\nu_e\nu_e} = 0.65$, the lower allowed limit from SN1987A [22]. The x here refers to all the six neutrino species.

reaction	A	B	C1	C2
$\nu_e + d \rightarrow p + p + e^-$	75	239	75	75
$\bar{\nu}_e + d \rightarrow n + n + e^+$	91	91	200	129
$\nu_x + d \rightarrow n + p + \nu_x$	544	544	544	544
$\bar{\nu}_e + p \rightarrow n + e^+$	255	255	423	314
$\nu_e + e^- \rightarrow \nu_e + e^-$	4.45	6.54	4.45	4.45
$\bar{\nu}_e + e^- \rightarrow \bar{\nu}_e + e^-$	1.54	1.54	2.09	1.73
$\nu_{\mu,\tau}(\bar{\nu}_{\mu,\tau}) + e^- \rightarrow \nu_{\mu,\tau}(\bar{\nu}_{\mu,\tau}) + e^-$	4.13	3.78	3.96	4.07
$\nu_e + {}^{16}O \rightarrow e^- + {}^{16}F$	1.39	61.60	1.39	1.39
$\bar{\nu}_e + {}^{16}O \rightarrow e^+ + {}^{16}N$	4.23	4.23	20.60	9.96
$\nu_x + {}^{16}O \rightarrow \nu_x + \gamma + X$	23.4	23.4	23.4	23.4

Figure Captions

Fig.1 The event rate as a function of time for the reaction (ν_x-d) in SNO for the scenario 1. The solid line corresponds to the case of massless neutrinos, the long dashed line to neutrinos with only mass but no mixing, while the short dashed line gives the event rate for neutrinos with mass as well as complete flavor conversion. The prompt burst neutrinos, undelayed for the no mixing case and delayed for the case of delay and mixing can be seen.

Fig.2 The ratio R(t) of the total charged current to neutral current event rate in SNO versus time for the scenario 1. The solid line is for massless neutrinos, the long dashed line for neutrinos with only flavor conversion but no delay, the short dashed line for neutrinos with only delay and no flavor conversion and the dotted line is for neutrinos with both delay and flavor conversion. The sharp dips in the ratio is due to conversion of the prompt burst ν_e to ν_μ when mixing is taken into account, which then are absent in the charged current but are present in the neutral current signal. The delayed and converted prompt ν_e burst is also visible.

Fig.3 Same as in Fig.1 but for the scenario 2.

Fig.4 Same as in Fig.2 but for the scenario 2.

Fig.5 Same as in Fig.2 but for neutrinos with inverted mass hierarchy with $m_{\nu_1} \ll m_{\nu_2} \sim m_{\nu_3} = 5eV$.

Fig.6 Same as in Fig.2 but for almost degenerate neutrinos ($m_{\nu_i} = 5eV$) with $m_{\nu_e} < m_{\nu_\mu} < m_{\nu_\tau}$.
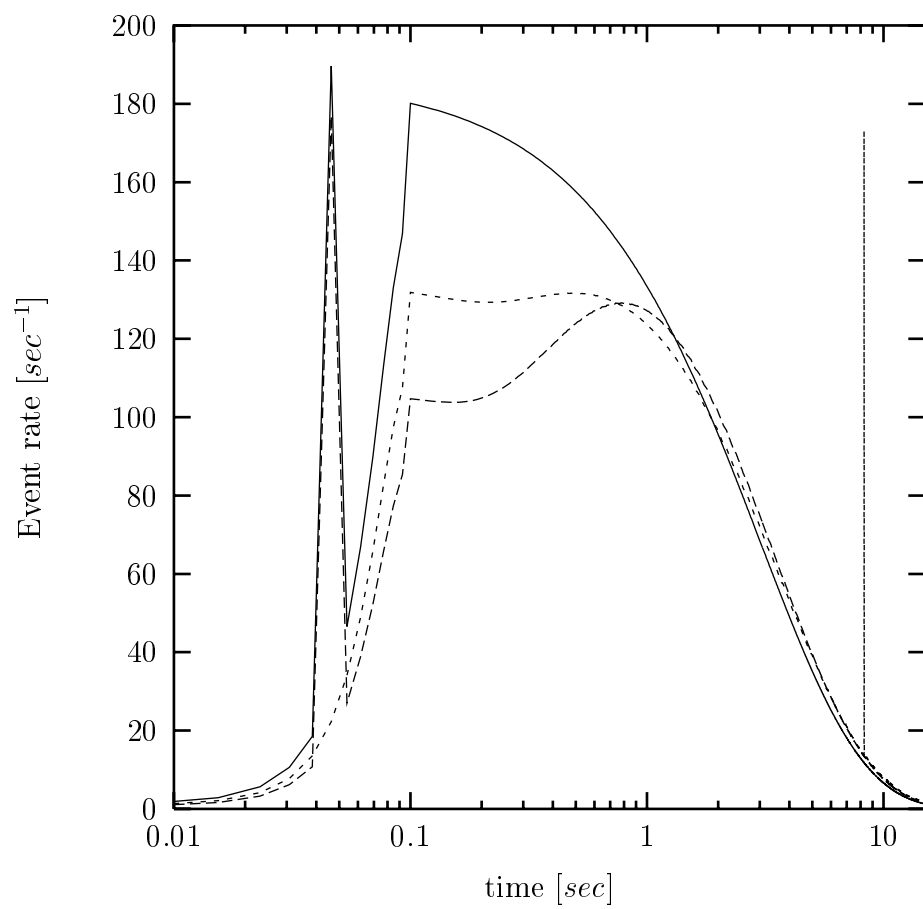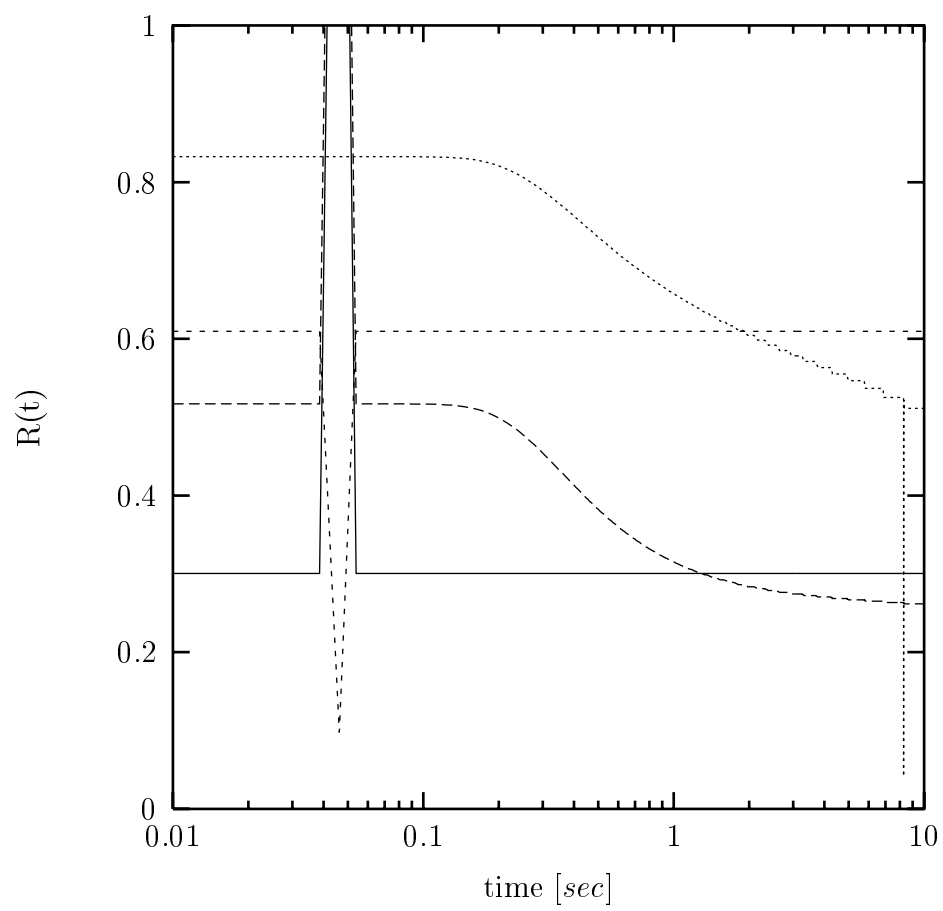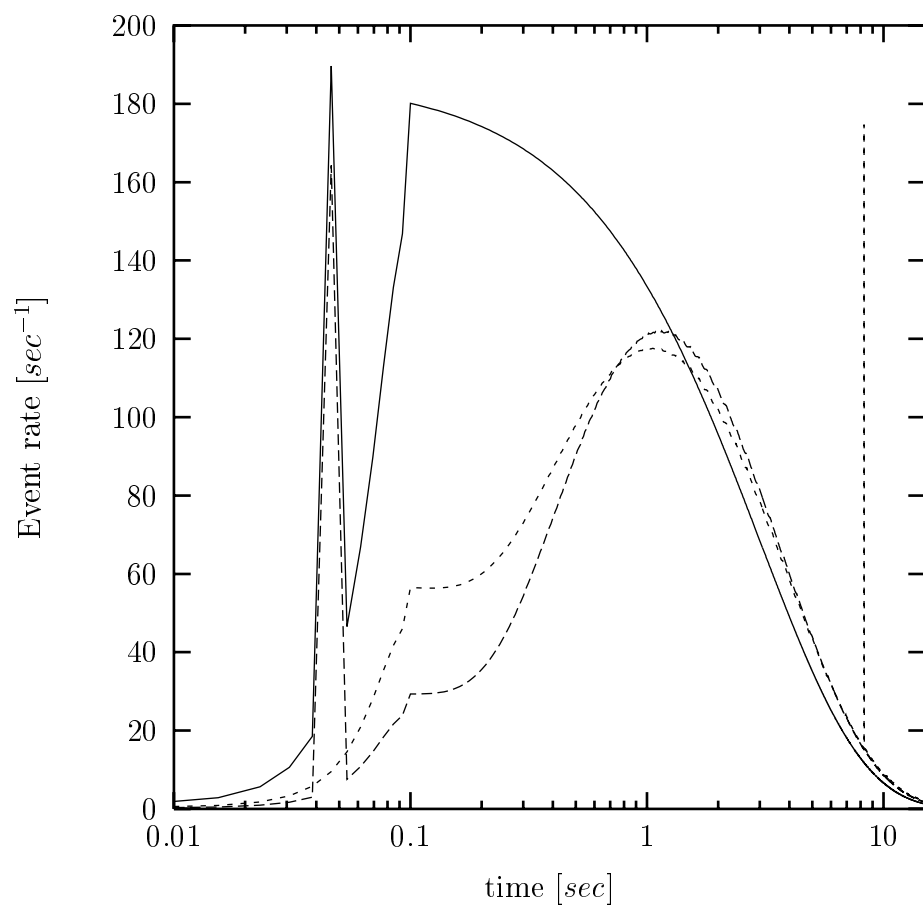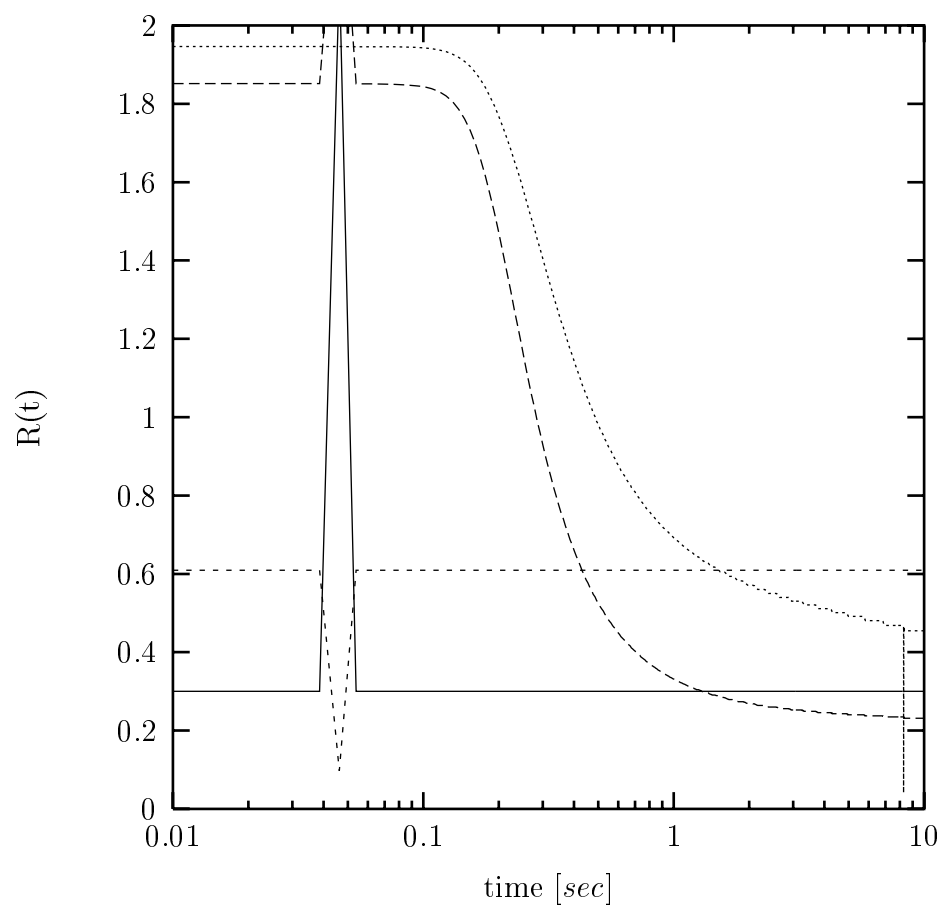
Fig.7 Same as in Fig.6 but for $m_{\nu_e} > m_{\nu_\mu} > m_{\nu_\tau}$.

Fig. 1

Fig. 2

Fig. 3

Fig. 4

Fig. 5

Fig. 6

Fig. 7